crystals

MDPI

Article

Carbonation of Sodium Aluminate/Sodium Carbonate Solutions for Precipitation of Alumina Hydrates—Avoiding Dawsonite Formation

Danai Marinos [1,*], Dimitrios Kotsanis [1], Alexandra Alexandri [1], Efthymios Balomenos [1,2] and Dimitrios Panias [1]

[1] Laboratory of Metallurgy, School of Mining and Metallurgical Engineering, National Technical University of Athens (NTUA), Heroon Polytechniou 9, 15780 Zografou, Greece; dkotsanis@metal.ntua.gr (D.K.); aalexandri@metal.ntua.gr (A.A.); efthymios.balomenos-external@alhellas.gr (E.B.); panias@metal.ntua.gr (D.P.)

[2] MYTILINEOS S.A, METTALURGY BUSINESS, Agios Nikolaos, 32003 Voiotia, Greece

* Correspondence: dmarinou@metal.ntua.gr; Tel.: +30-210-772-2299

Abstract: Experimental work has been performed to investigate the precipitation mechanism of aluminum hydroxide phases from sodium aluminate/sodium carbonate pregnant solutions by carbon dioxide gas purging. Such solutions result from leaching calcium aluminate slags with sodium carbonate solutions, in accordance with the Pedersen process, which is an alternative process for alumina production. The concentration of carbonate ions in the pregnant solution is revealed as a key factor in controlling the nature of the precipitating phase. Synthetic aluminate solutions of varying sodium carbonate concentrations, ranging from 20 to 160 g/L, were carbonated, and the resulting precipitating phases were characterized by X-ray diffraction analysis. Based on the results of the previous carbonation tests, a series of experiments were performed in which the duration of carbonation and the aging period of the precipitates varied. For this work, a synthetic aluminate solution containing 20 g/L free Na_2CO_3 was used. The precipitates were characterized with X-ray diffraction analysis and Fourier-transform infrared spectroscopy.

Keywords: precipitation; aluminum hydroxide; dawsonite; sodium aluminate solution; carbonation; Pedersen process; bayerite; CO_2 purging

Citation: Marinos, D.; Kotsanis, D.; Alexandri, A.; Balomenos, E.; Panias, D. Carbonation of Sodium Aluminate/Sodium Carbonate Solutions for Precipitation of Alumina Hydrates—Avoiding Dawsonite Formation. *Crystals* **2021**, *11*, 836. https://doi.org/10.3390/cryst11070836

Academic Editor: Béatrice Biscans

Received: 23 June 2021
Accepted: 16 July 2021
Published: 20 July 2021

1. Introduction

Currently, the dominant process to produce metallurgical grade alumina is the Bayer process. With the Bayer Process, high-quality bauxites are digested in caustic solutions to selectively dissolve the aluminum hydroxide content of the ore. The resulting aluminate solution is supersaturated in aluminum trihydroxide, which is precipitated through seeding precipitation, which takes advantage of the temperature dependence of aluminum trihydroxide solubility in alkaline solutions. A major drawback of the process is the excessive production of the solid residue of the leaching stage, the so-called bauxite residue, which contains all the unreacted components of the original ore, as well as phases that have precipitated during the caustic digestion step. Practically, the ratio of alumina to residue production is equal to one [1]. Alternatives to the Bayer process have been studied in the past, and the Pedersen process is one of them, which was applied in the Høyanger plant in Norway from 1929 to 1969 with an annual production of about 17,000 tons of alumina [2,3]. Although the Pedersen process was abandoned in 1969, studying the process from the perspective of sustainability and circular economy, several advantages stand out [4]. Primarily, it promises a complete utilization of bauxite ores, even some rejected by the Bayer process [5–7], since it aims at the production of iron and alumina. Of course, the process also faces some limitations in terms of the type of raw material: if the raw material contains more than 44% of Al_2O_3, then the amount of SiO_2 cant exceed 8% [5], and also,

the process will not be economically viable if the iron content is very low. Moreover, a benefit of the Pedersen process is that the hydrometallurgical conditions employed are moderate and, most importantly, the issue of bauxite residue is eliminated as, in its place, a calcium-based residue is produced in the leaching stage with potential applications.

In the Pedersen process, prior to leaching, bauxite ore (of suitable Fe concentration) is reductively smelted in an Electric Arc Furnace (EAF) with fluxes, mainly lime, to recover the metallic iron and produce a calcium aluminate slag [3,7–10]. In this stage, it is important to produce a slag of appropriate crystallinity and chemical composition, that will be easily soluble in the subsequent leaching step [7]. In the leaching step, the slag is leached with a dilute sodium carbonate/sodium hydroxide solution to produce a calcium carbonate residue (called grey mud) and a pregnant sodium aluminate solution (PLS) [8–12]. Following a solid/liquid separation process, the pregnant solution enters the precipitation stage, where carbon dioxide gas is bubbled to lower the pH of the solution and precipitate aluminum as aluminum trihydroxide [8–10,12,13]. Carbon dioxide is dissolved in the sodium aluminate solution according to Reactions (1) and (2) [12,14–16]. With the increase in hydrogen ion concentration, resulting from the dissolution of CO_2, the alkaline solution is gradually neutralized, reducing the pH and triggering the decomposition of the aluminate ion, resulting in the precipitation of aluminum hydroxide according to Reaction (3) [14–16].

$$CO_2 + H_2O = HCO^-_{3(aq)} + H^+_{(aq)} \quad (1)$$

$$HCO^-_{3(aq)} = CO^{2-}_{3(aq)} + H^+_{(aq)} \quad (2)$$

$$Al(OH)^-_{4(aq)} = Al(OH)_{3(s)} \downarrow + OH^-_{(aq)} \quad (3)$$

Concerning the Pedersen process, the pyrometallurgical stage has been extensively studied, and plenty of information is available in the literature. On the contrary, the literature concerning the hydrometallurgical stage and especially the precipitation stage of the process is quite limited.

The patents of the Pedersen process [9,10] initially declared that carbon dioxide precipitation is feasible but not effective. Later, it was claimed that, by adding sodium hydroxide to increase alkalinity and alumina hydrate seed, precipitation can be performed at 80 °C according to the principles of the Bayer precipitation stage. The spent solution after precipitation is then recarbonated with carbon dioxide gas and recycled to the leaching stage. Additionally, knowledge on the Pedersen process provided by a report from the Bureau of Mines [12] indicates that the resulting PLS from the Pedersen process contained 15–20 g/L of Al_2O_3 and the precipitation lasted for 10–15 h without clarifying whether the duration mentioned only refers to the carbonation period or to both the carbonation and the aging period.

Information is also available by some research groups that have attempted to modify the Pedersen process by changing the composition of the leaching solution or by using the process with alternate raw materials (e.g., clay instead of bauxite or other types of bauxites). These research groups applied carbonation temperatures ranging from 50 to 90 °C. Henry E. Blake et al. [17] ended the carbonation at a pH of 9.5, at 70 °C, precipitating 93% of aluminum (with 17–28% losses in the desilication step) as alumina hydrate. T. P. Hignett [8] presented a pilot plant operation, in which carbonation took place at 50–70 °C for 10 to 30 h, also applying a 2 h aging stage. Thomson et al. [12] mention that the sodium aluminate solutions resulting from leaching are unstable. Precipitation stopped at a pH of 10.8 at 80 °C with a duration of 4–8 h. Additionally, this patent [11] carried out the precipitation at 90 °C following the approach of the Pedersen patents.

Besides being mentioned in the Pedersen process, precipitation by carbonation is highly attractive to alumina refineries that operate based on sintering processes, since the neutralized product of sodium carbonate can be directly recycled. Such is the case in refineries in Russia and China that have poor grade diasporic bauxites or nepheline [18–20]. The ore is mixed with Na_2CO_3 and is sintered in temperatures higher than 1000 °C to

form sodium aluminate, which is highly soluble in water. Out of such aluminate solutions, alumina hydrates are precipitated by carbonation [21]. The carbonation process is carried out in temperatures of room temperature (RT) to 80 °C [14–16,22–24] and duration times ranging from 5–8 h [25]. Lee et al. [26] showed that higher temperatures (70 °C) favor the formation of gibbsite, while lower temperatures (RT) favor the formation of bayerite. Padilla et al. [22] carried out the carbonation at RT, precipitating 97% of Al as boehmite and 20% of the silicon. Shayanfar and Aghazadeh et al. [14–16] carried out extensive research on the carbonation of aluminate solutions resulting from the nepheline lime-sinter process. Both thermodynamically and experimentally, they have shown that at an ending pH of 9, 10 and 11, dawsonite, a mixture of dawsonite and imogolite and bayerite, correspondingly, are precipitated.

Apparently, the carbonation of sodium aluminate solutions is a process not sufficiently understood, as suggested by the literature review that was presented, concerning: the composition of the PLS undergoing precipitation is not always mentioned, temperature can range from RT to 90 °C, ending pH from 9.5 to 11, gas composition (% of CO_2 in gas), the gas flow rate, stirring, reactor design, the phases precipitating mentioned are not always the same, etc. [9–12,14–19,23,24,27]. The focus of the current work is to understand the effect of the concentration of unreacted sodium carbonate that remains from the leaching step and how it affects the type/composition of the precipitates and at the same time to maximize the recovery of aluminum in the form of alumina hydrates in synthetic sodium aluminate/sodium carbonate solutions.

2. Materials and Methods

Synthetic solution preparation: To study the precipitation mechanism, synthetic solutions resembling the solutions generated by leaching the calcium aluminate slags with sodium carbonate solution had to be prepared. The reagents used to prepare the aluminate solution were: NaOH pellets, Na_2CO_3 anhydrous for analysis, technical grade sodium aluminate ($NaAlO_2$) and technical grade anhydrous sodium metasilicate (Na_2SiO_3). Depending on the desired final concentration of the solution, the reagents were mixed in deionized water and the solution was added in a 1 L volumetric flask. The solution was then filtered to remove any impurities and the resulting solution was analyzed with Atomic Absorption Spectroscopy (AAS), (PinAAcle 900T, Perkin Elmer, Waltham, MA, USA) to determine the concentration of Al and Si. The composition of the starting aluminate solution is given in Table 1. The NaOH concentration is always 18.75 g/L, while the concentrations of free Na_2CO_3, Al and Si varied between 20 and 160 g/L, 8 and 8.5 g/L and 0.2 and 0.24 g/L, respectively. The initial and final solutions in all experiments were analyzed for their Al and Si content.

Table 1. Concentration of synthetic sodium aluminate solution.

Compound	Starting Synthetic Solution to Precipitation (g/L)
Na_2CO_3	20, 40, 60, 80, 160
NaOH	18.75
Al	8–8.5
Si	0.2–0.24

Carbonation experiments: The experiments were conducted with the experimental setup shown in Figure 1, which is a custom-made autoclave system by AMAR. The reactor (1) is made of Inconel 625 to resist highly alkaline solutions and has a 1.8 L working volume. It uses an electrical ceramic band for heating and a $\frac{1}{4}$ hp AC motor for stirring controlled by the controller (2). Additionally, the vessel is equipped with baffles and a serpentine cooling coil. The reactor has a flush-bottom valve to unload the final pulp. The head of the reactor has a CO_2 gas inlet, an outlet, a motorhead stirrer, an opening for sampling or for the pH electrode, a cooling coil inlet and outlet, a thermocouple inlet, and a funnel to insert solid or liquid samples. The pH is monitored and recorded by an Endress and Hauser measuring

system (3). The gas flow rate is controlled with a 0–500 mLn/min mass flowmeter by Bronkhorst controlled by computer software (4). Apart from the resistance heating, cooling or heating can be also controlled by a chiller (5) recirculating liquid through the cooling coil. Pure carbon dioxide gas (99.995% purity) was used throughout all the experiments. The pH was monitored, through a pH electrode by Endress and Hauser, inserted into the solution, equipped with a pH recorder, using a 1 min step.

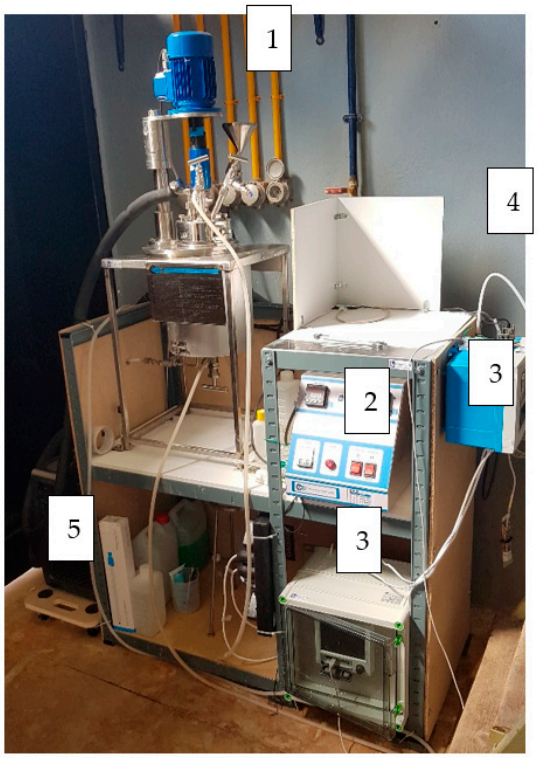

Figure 1. Precipitation reactor-experimental setup.

A volume of 800 mL of the starting synthetic solution was introduced through the reactor's built-in funnel and heated to 40 °C. When the desired temperature was reached, CO_2 gas was injected at a constant flow rate of 160 mLn/min. The stirring rate was set at 200 rpm. At the end of the experiment (predesigned time and aging period), the solution was un-loaded and filtered. The filtrate was analyzed by AAS to determine the concentration of Al and Si after precipitation. The solid precipitate was dried at 110 °C for 24 h and then it was analyzed by X-ray diffraction (XRD) on an X'Pert Pro diffractometer (PANalytical) with CuKa radiation (diffraction patterns were recorded between 10 and 70° 2θ, in 0.02° steps and 2 s per step) and Fourier-transform infrared spectroscopy (FT-IR) on a PerkinElmer Spectrum 100 spectrometer, equipped with a diamond attenuated total reflectance (ATR) accessory (spectra were acquired in transmittance mode, from 4000 cm^{-1} to 650 cm^{-1} with a resolution of 4 cm^{-1} and 16 scans per spectrum).

3. Results

3.1. Effect of Initial Sodium Carbonate Concentration

The examined concentrations of Na_2CO_3 in the starting solution were 20, 40, 60, 80, 100, and 160 g/L, as shown in Table 1. The carbonation time was set arbitrarily to 70 min and no aging period was employed. Figure 2 depicts the XRD graphs obtained by the powder XRD examinations of the precipitates from each experiment. At 20 g/L of sodium carbonate in the starting solution, boehmite is the only precipitating phase; the broad peaks indicate a poorly crystalline phase with small particle size [28]. A better-crystallized bayerite is coprecipitated along with boehmite at 40 g/L of sodium carbonate in the starting solution Crystal structures and X-ray powder diffraction data can be found

in Supplementary Materials: Figure S1, Table S1, Figure S2 and Table S2. At 60 g/L of sodium carbonate in the starting solution, boehmite and bayerite are precipitated, but the main peak of dawsonite (at about 15.5) can also be observed in the XRD graph. At 80 and 100 g/L of sodium carbonate in the starting solution, dawsonite is precipitated along with bayerite and boehmite. At 160 g/L of sodium carbonate in the starting solution, only dawsonite can be observed in the XRD graph.

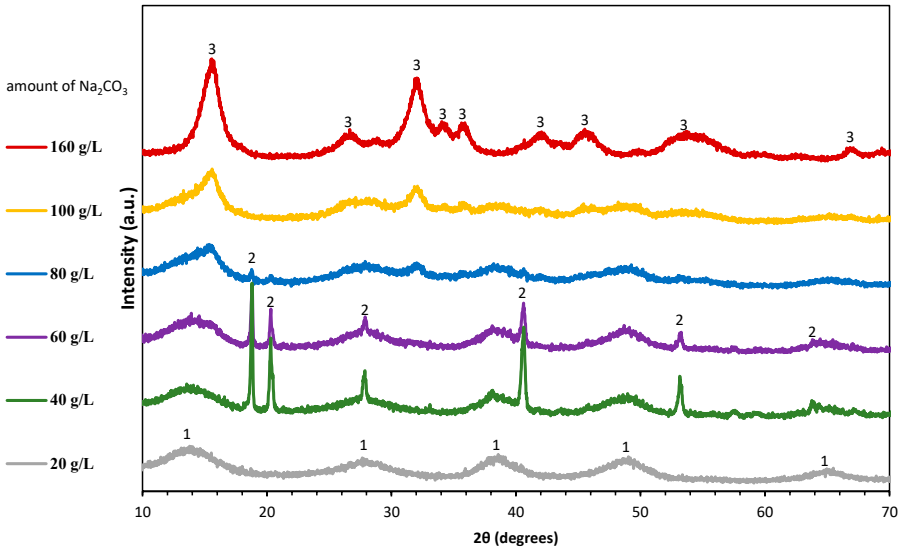

Figure 2. XRD graphs of precipitates of carbonation in sodium aluminate solutions of different starting concentration of Na_2CO_3 [carbonated at 40 °C, 160 mLn/min CO_2 flow rate, 70 min carbonation time and 200 rpm stirring. No aging period]. 1—Boehmite [AlOOH], 2—Bayerite [$Al(OH)_3$], 3—Dawsonite [$NaAlCO_3(OH)_2$].

The results presented above, show that the initial free sodium carbonate concentration affects substantially the type of phases that are precipitated. Dawsonite is gradually increased until it becomes the dominating precipitated phase by increasing the initial free sodium carbonate concentration in the solution. Dawsonite is not present at the precipitating phases up until the 60 g/L amount of sodium carbonate concentration in the starting solution. As the goal of this research is to produce pure alumina hydroxides, the concentration of 20 g/L of sodium carbonate in the starting solution was chosen as the starting condition for further optimization.

3.2. Effect of Carbonation Duration

To elucidate the precipitation mechanism during carbonation of sodium aluminate solutions with low free sodium carbonate content (20 g/L), experiments were performed at 40 °C, with a 200 rpm stirring rate and 160 mL/min CO_2 flow rate varying in duration without an aging period at the end of carbonation. The values of duration that were chosen are as follows: 30, 45, 60, 70, 80, 90, 110, and 205 min. The values of the pH of the solution/pulp along with the corresponding Al recovery against the duration carbonation can be seen in Figure 3. In Figure 4, the XRD graphs of the precipitates obtained from each experiment are shown.

In region I (30 min of carbonation), the system exhibits high buffering capacity, and the pH value gradually decreases. In this region, the free hydroxide ions concentration is high, and therefore, the acidity produced by the dissolved CO_2 through Reactions (1) and (2) is consumed, slightly lowering the pH value of the solution. In region I, not enough mass of precipitate was obtained to perform XRD or FTIR analysis. In region II (30–45 min of carbonation), the solution buffer capacity is substantially lower, and therefore, the acidity produced by the added CO_2 sharply decreases the solution pH. In this region, aluminum precipitation has already started, precipitating boehmite (22%

recovery, at 45 min of carbonation). In region III (45–60 min of carbonation), the solution exhibits remarkably high buffering capacity again, which can be attributed to the massive aluminum precipitation, according to Reaction (4), that again liberates free hydroxide ions consuming the protons generated by the added CO_2. In this region, aluminum is precipitated as boehmite again (41% recovery, at 60 min of carbonation). Finally, in region IV (>60 min of carbonation), the value of the pH is gradually decreased again until the end of precipitation. In general, aluminum recovery expressed as % of Al precipitated out of the solution, which increases as more carbon dioxide is added (Figure 3), showing a sigmoid curve with negligible aluminum precipitation in region I, very low in region II, low to medium in region III and medium to high in region IV.

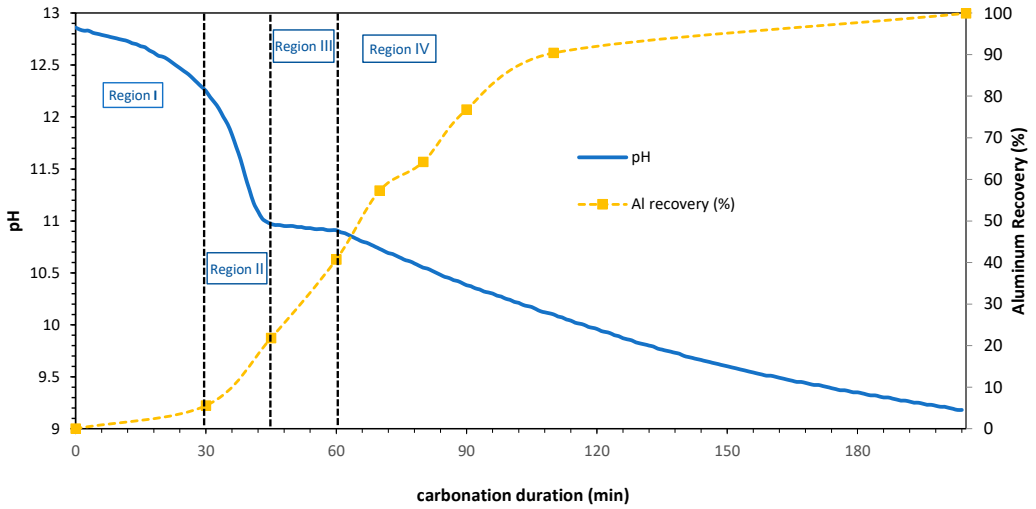

Figure 3. Graph representing the pH and the aluminum recovery (%) in the precipitate vs. the carbonation duration. [Sodium aluminate solution that contains 20 g/L sodium carbonate, carbonated at 40 °C, 160 mLn/min CO_2 flow rate and 200 rpm stirring. No aging period.].

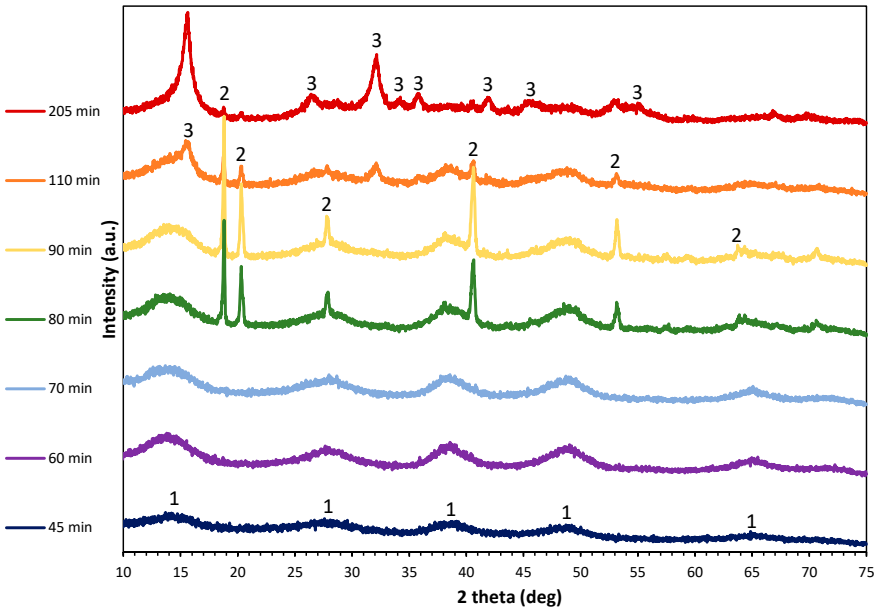

Figure 4. XRD graphs of precipitates [Sodium aluminate solution that contains 20 g/L sodium carbonate, carbonated at 40 °C, 160 mLn/min CO_2 flow rate and 200 rpm stirring. No aging period.]. 1—Boehmite [AlOOH], 2—Bayerite [$Al(OH)_3$], 3—Dawsonite [$NaAlCO_3(OH)_2$].

$$Al(OH)^{-}_{4(aq)} = AlOOH_{(s)} + OH^{-}_{(aq)} + H_2O_{(l)} \quad (4)$$

In more detail, as seen in Figure 4, between 45 and 70 min of carbonation (pH 10.96–10.73), boehmite is the only precipitating phase corresponding to recovery up to 57.28% of Al. From 70 to 90 min of carbonation (pH 10.73–10.38), boehmite along with bayerite are precipitated, corresponding to a recovery of Al up to 77%. At 110 min of carbonation and afterward, dawsonite is the major precipitate, with bayerite and boehmite as minor phases, achieving an almost complete recovery of aluminum in the precipitate (~100%).

3.3. Effect of Aging

The tests conducted in Section 3.2 were reproduced, this time with the inclusion of aging as a parameter. Aging durations of 2, 4, and 24 h was tested. Upon completion of the carbonation process, CO_2 gas purging stopped, and the pulp formed during precipitation was kept in agitation under temperature with predefined aging duration. At the end of the aging period, the precipitates were characterized with XRD, and the solution was analyzed for its Al and Si content. Al recoveries for different aging durations in the precipitate can be observed in Figure 5a, while the corresponding Si recoveries are observed in Figure 5b. Additionally, the XRD diffractograms are presented in Figure 6.

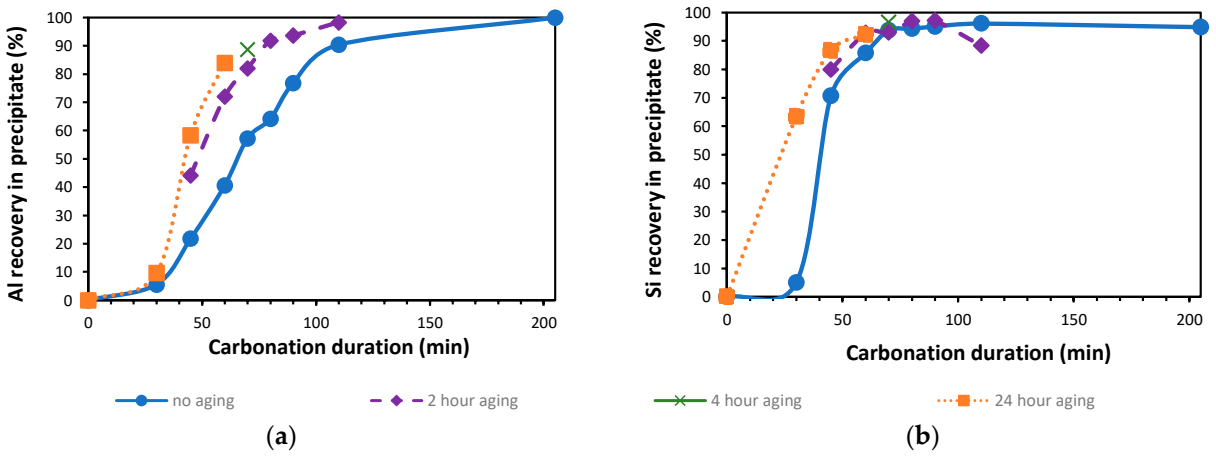

Figure 5. (**a**) Aluminum recovery in precipitate vs carbonation time. (**b**) Silicon recovery in precipitate vs carbonation duration. Aging period of 0, 2, 4 or 24 h. [Sodium aluminate solution that contains 20 g/L sodium carbonate, carbonated at 40 °C, 160 mLn/min CO_2 flow rate and 200 rpm stirring].

At 30 min of carbonation and a 24 h aging period, 10% of Al and 63% of Si was precipitated, but only a very small amount of precipitate could be obtained, and thus XRD analysis could not be performed. Instead, FTIR analysis was performed, which mainly identified a sodium zeolite phase.

The experiment at 45 min resulted in an aluminum recovery increase from 22% to 44% at 2 h aging and 58% at 24 h aging. At 60 min of carbonation, the aluminum recovery increased from 41% to 72% at 2 h of aging and 84% at a 24 h aging period. From 45 to 60 min of carbonation, boehmite was initially precipitated, which during aging was transformed to bayerite. At 70 min of carbonation, aluminum recovery boosted from 57% to 82% at a 2 h aging period and 89% at a 4 h aging period. Though, at 4 h of aging, dawsonite was also precipitated. The following experiments showed an increase in aluminum recovery during aging again, but the precipitating phase was always dawsonite after aging, as depicted in Figure 6.

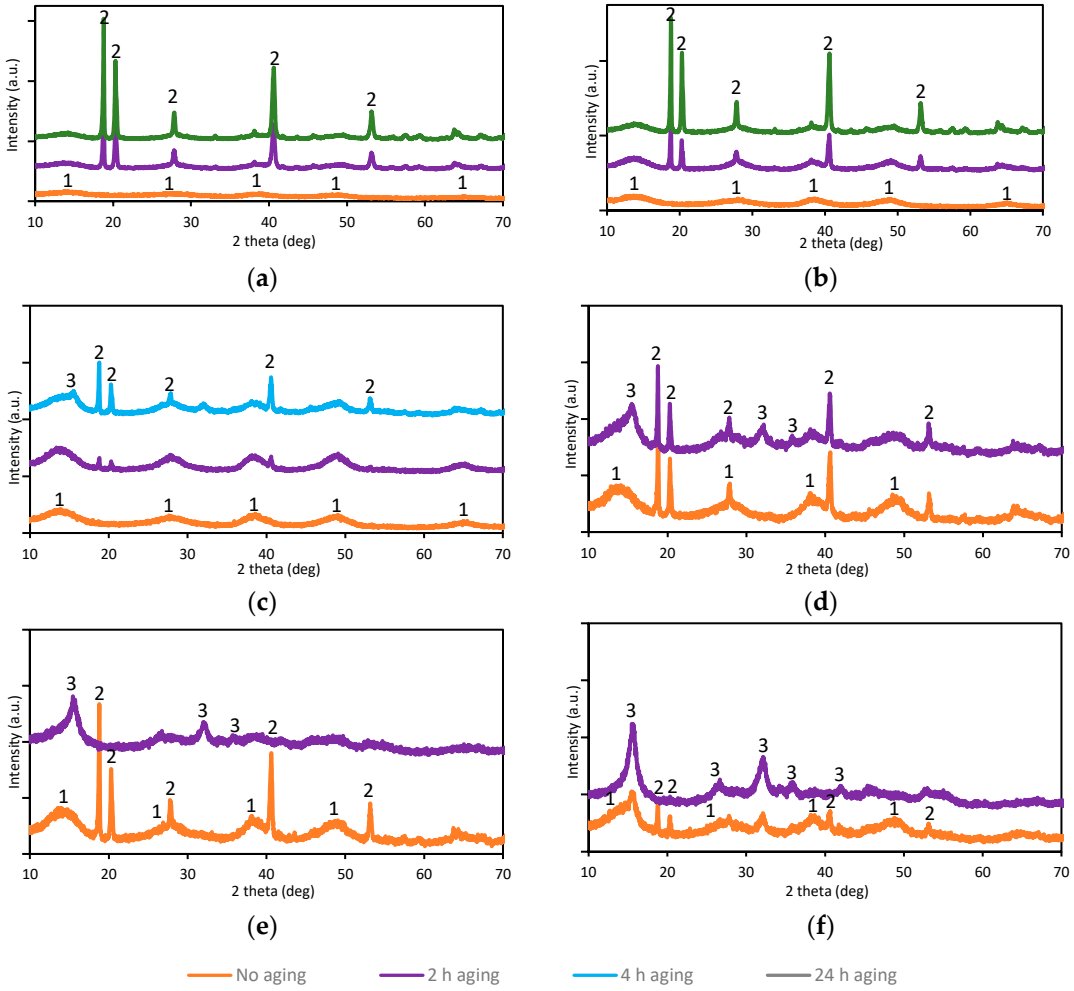

Figure 6. XRD graphs of precipitates. Carbonation period of (**a**) 45 min, (**b**) 60 min, (**c**) 70 min, (**d**) 80 min, (**e**) 90 min, (**f**) 110 min Aging period of 0. 2, 4 or 24 h. [Sodium aluminate solution that contains 20 g/L sodium carbonate, carbonated at 40 °C, 160 mLn/min CO_2 flow rate and 200 rpm stirring]. 1—Boehmite [AlOOH], 2—Bayerite [$Al(OH)_3$], 3—Dawsonite [$NaAlCO_3(OH)_2$].

Overall, silicon has a higher precipitation rate than aluminum, as seen in Figure 5b. Silicon precipitation starts earlier than aluminum precipitation, which serves as a desilication step. Almost all the silicon was co-precipitated, a result that is in accordance with the work of previous authors [2,9,10,17].

In general, in all cases after the end of the aging period, the recovery of aluminum was higher than the corresponding recovery obtained without aging. The results show slow alumina hydrate formation kinetics during carbonation, indicating that the system under investigation requires a sufficiently long aging period in order to precipitate as much of the aluminum as possible. This shows the necessity of applying aging for the process designed.

Furthermore, all precipitates were analyzed with FTIR spectroscopy. A typical graph of the precipitate obtained with an initial concentration of 20 g/L sodium carbonate, carbonation time of 60 min at 40 °C, 160 mLn/min CO_2 flow rate, and 200 rpm stirring is shown in Figure 7 and the FTIR data in Table 2. It can be observed that the major phase is bayerite (identified in wavenumbers: 3656, 3550, 3462, 3438, 3429, 1021, 981 and 718 cm^{-1}) along with boehmite (identified in wavenumbers: 3316 and 3096 cm^{-1}) as a minor phase, as was expected from the XRD analysis. Apart from these phases, a phase termed aluminum hydroxide carbonate gel (identified in wavenumbers: 1523 and 1406 cm^{-1}), which is an amorphous phase, was also present in the precipitate. According to the literature [29,30],

aluminum hydroxide carbonate gel presence is usually accompanied by adsorbed water, which was also observed on the FTIR analysis. Gel formation could be a result of the rapid precipitation, as it is well known from the literature [31,32] that carbonates contribute to maintaining aluminum hydroxide gel in the amorphous form. When aluminum hydrolysis is performed in the presence of CO_2, the resulting carbonates are specifically adsorbed on aluminum hydroxide gel, stabilizing it in the form of aluminum hydroxycarbonate gel (Reaction (5)) which retains its gelatinous nature even upon aging and does not contain other cations except those of aluminum [30].

$$Al(OH)_{3(gel)} + xCO_3^{2-} = Al(OH)_{(3-2x)}(CO_3)_{x(gel)} + 2xOH^- \quad (5)$$

It is suggested that aluminum hydroxycarbonate gel is the amorphous form of scarbröite, which is a crystalline phase of aluminum hydroxycarbonate, $Al(OH)CO_3$ [29]. Therefore, the first precipitate in the presence of CO_2 gas will always contain a small amount of aluminum hydroxycarbonate gel, as it is seen also in this work under all studied experimental conditions. Additionally, adsorbed water was observed at 1651 cm^{-1}.

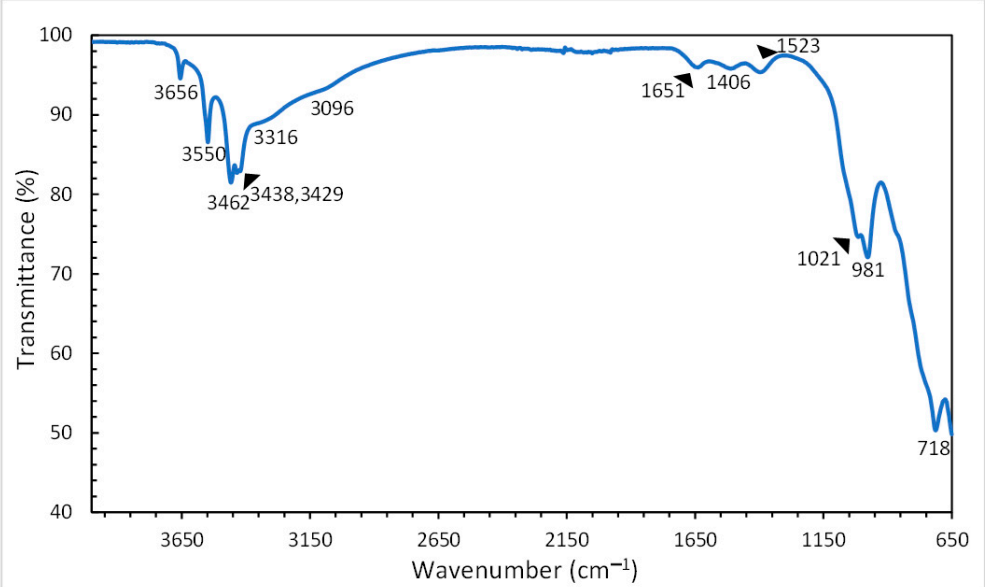

Figure 7. FTIR graph of precipitate obtained with initial concentration of 20 g/L sodium carbonate, carbonated at 40 °C, 160 mLn/min CO_2 flow rate, 200 rpm stirring and 24 h aging period].

Table 2. FTIR data (Functional group/vibration type, attributed phases and references).

Attributed Phase	Wavenumber (cm^{-1})	Functional Group/Vibration	References
Bayerite	3656, 3550, 3462, 3438, 3429	O–H stretching band	[33–39]
	1021, 981	O–H bending band	[33,35–37]
	718	Al–OH vibration	[33,36]
Aluminum hydroxide carbonate gel	1523, 1406	CO_3^{-2} asymmetric stretching band	[32,40,41]
Boehmite	3316, 3096	O–H stretching band	[32,35,37,42–44]
Adsorbed water	1651	H–O–H bending	[30,37,38,44,45]

4. Discussion

Based on the author's knowledge of the alumina hydrate precipitation in aluminate solutions [46], the following hypothesis is proposed as an explanation for the experimental observations: as the bubbles of CO_2 gas are added in the highly alkaline sodium aluminate/sodium carbonate solution, the neutralization of hydroxide ions is performed, and thus the solution pH is gradually decreased. Locally, in the area around the CO_2 gas bubble

(Figure 8), a low pH area due to acidity imposed by the CO_2 gas dissolution is established, instantly causing the formation of boehmite (Reaction (6)), as it has been shown in previous work [47]. In addition, the vigorous agitation transfers the protons through convection to the bulk solution, which is strongly alkaline and thus promotes a bayerite formation [22] according to Reaction (7). Boehmite precipitation has also been observed by only two research groups [6,48].

$$Al(OH)^{-}_{4(aq)} + H^{+}_{(aq)} = AlOOH_{(am)} + 2H_2O_{(l)} \quad (6)$$

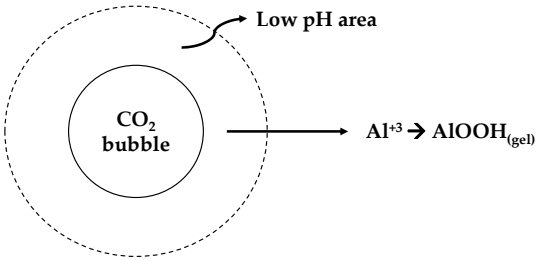

Figure 8. Schematic representation of boehmite precipitation.

Then, during aging, as the CO_2 bubbling stops, the above-stated low pH area cannot be established, and thus boehmite cannot be precipitated. On the contrary, and as the solution is still oversaturated, bayerite starts precipitating [46] according to Reaction (3) as under those conditions, (mild to strong alkaline environment) is the most stable phase.

Therefore, the initial precipitates always contain boehmite and bayerite. During the aging period, bayerite is precipitated as the solution is still oversaturated, while boehmite, formed during carbonation, is gradually transformed to the stable alumina hydrate (bayerite), which is in the thermodynamically stable phase at 40 °C under the alkaline conditions prevailing in the solution [49–51] following Reaction (7).

$$AlOOH_{(am)} + H_2O = Al(OH)_{3(s)} \quad (7)$$

On the other hand, the hydrolysis of aluminum in the presence of at least stoichiometric amounts of sodium bicarbonate (pH less than around 10) leads to the formation of dawsonite [15,32] according to Reaction (8). This is also observed in this work for the first precipitates with no aging period at 110 min of carbonation, where dawsonite is initially precipitated and the pH value is remarkably close to 10.

$$Al(OH)^{-}_{4} + NaHCO_{3(aq)} = NaAl(OH)_{(2)}(CO_3)_{(s)} + OH^{-} + H_2O \quad (8)$$

In summation, the aluminum recoveries, the pH values, and the time derivative of pH ($\frac{dpH}{dt}$, which denotes as ΔpH) are shown in Figure 9 and Table 3, where, based on the precipitating phases, now, five broad regions can be distinguished. Region I is where a sodium zeolite phase starts to precipitate with Al recovery up to 10%, while the derivative of pH ranges from 0.01 to -0.04, showing a slow decrease in pH. This is the region that relates to the neutralization of hydroxide ions. In region II, alumina hydrate phases start to precipitate with Al recovery up to 58%, along with a pH gradient as high as 0.15 and a decrease in pH. In this region, most of the hydroxide ions have been neutralized. Moving on, region III is where alumina hydrates are precipitated, with recovery up to 84% after aging (first boehmite is precipitated which transforms to bayerite during aging) and the ΔpH ranges from 0 to -0.01 showing an almost steady pH. In this region, the acidity produced by the addition of CO_2 gas is neutralized by the alkalinity produced from the massive precipitation of aluminum. The following region, region IV, represents that stage of carbonation where metastable alumina hydrates are precipitated (first, boehmite is precipitated which is then transformed to bayerite during aging, and finally, a sufficient

period of aging is induced) with a recovery of Al up to 94%. Finally, in region V, dawsonite is precipitated, initially reaching a recovery of Al up to 100%. In this region, the pH decreases with a ΔpH of −0.01 to −0.02 initially, and of 0 to −0.01 after 158 min.

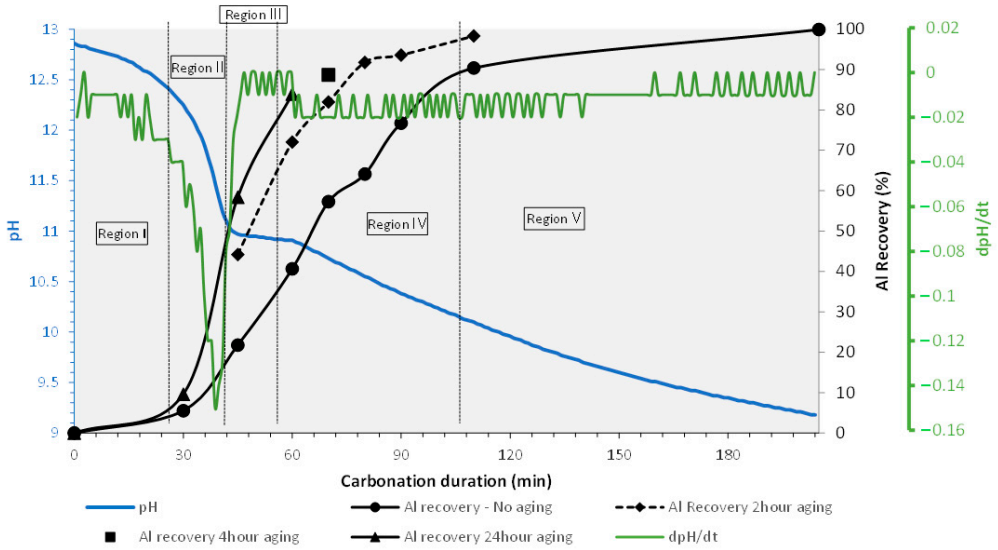

Figure 9. Graph representing the pH during carbonation, the aluminum recovery, and the time derivative of pH (dpH/dt) vs carbonation duration (min). [Sodium aluminate solution that contains 20 g/L sodium carbonate, carbonated at 40 °C, 160 mLn/min CO_2 flow rate and 200 rpm stirring].

Table 3. Distinguished regions, aluminum recovery (%) and ΔpH.

Region	Phase Precipitating	Maximum Al Recovery (%) in Precipitate after Aging	Range of Dph/Dt
I	Sodium zeolite	10%	0 to −0.03
II	Alumina hydrates	58%	−0.04 to −0.15
III	Alumina hydrates	84%	0 to −0.01
IV	Metastable alumina hydrates	94%	0.01 to 0.02
V	Dawsonite	100%	0 to −0.02

5. Conclusions

The concentration of sodium carbonate in the sodium aluminate pregnant solution is an important factor for the precipitation stage to obtain $Al(OH)_3$ through the carbonation process. At concentrations lower than 40 g/L of Na_2CO_3, alumina hydrates (boehmite and bayerite) are precipitated, whereas at concentrations higher than 60 g/L of Na_2CO_3, dawsonite is co-precipitated, and as the free sodium carbonate concentration increases, it becomes the predominant precipitated phase.

In general, a solution with 20 g/L of sodium carbonate can precipitate alumina hydrates in the form of crystalline bayerite with a maximum recovery of 84%. This was achieved under carbonation at 40 °C with 60 min CO_2 purging with pure CO_2 gas and a flow rate of 160 mLn/min after a 24 h aging period. It was shown that first, boehmite precipitates, during aging, transform to bayerite and if the carbonates content increases, into dawsonite. Silicon is always co-precipitated with aluminum and should be carefully monitored in the leaching step. Desilication can happen at the first stages of solution carbonation but leads to some alumina losses in the order of 10%.

Additionally, five broad areas were recognized based on the pH trendline and results of region I, relating to the neutralization of hydroxide ions, where silicon has started a bulk precipitation. In region II, where most of the hydroxide ions have been neutralized, alumina hydrate phases start to precipitate with Al recovery up to 58%. Moreover, region

III is where alumina hydrates are precipitated with recovery up to 84%. The following region, region IV, represents that stage of carbonation where metastable alumina hydrates are precipitated (first, boehmite is precipitated, which is then transformed to bayerite during aging and finally to dawsonite if a sufficient period of aging is induced), with a recovery of Al up to 94%. Finally, in region V, dawsonite is precipitated, initially reaching a recovery of Al up to 100%.

Overall, key parameters were determined and helped improve the general knowledge of precipitation of sodium aluminate solutions with carbon dioxide. Unreacted sodium carbonate content from the leaching step was one of the key parameters tested and the precipitation pathway was revealed, showing that boehmite is first precipitated, followed by bayerite and finally dawsonite if the carbonate content is high enough. A lot of future work is needed in order to more carefully specify the exact consistency of the solution when dawsonite starts to form, and of course to produce metallurgical grade alumina, other properties such as purity, appropriate particle size, etc., need to be investigated.

Supplementary Materials: The following are available online at https://www.mdpi.com/article/10.3390/cryst11070836/s1, Figure S1: Crystal structure of boehmite. PDF 04-016-2858, Table S1: X-ray Powder Diffraction data for boehmite. PDF 04-016-2858, Figure S2: Crystal structure of bayerite. PDF 01-074-1119, Table S2: X-ray Powder Diffraction data for bayerite. PDF 01-074-1119. Reference [52] is cited in supplementary materials.

Author Contributions: Conceptualization, D.M., D.P. and E.B.; methodology, D.M., D.P. and E.B.; software, D.M. and D.K., data curation, D.M.; D.K. and A.A.; writing—original draft preparation, D.M.; writing—review and editing, D.M., D.P., D.K. and E.B.; visualization, D.M., D.P. and E.B.; supervision, D.P. and E.B.; project administration, D.P. All authors have read and agreed to the published version of the manuscript.

Funding: The research leading to these results has received funding from the European Community's Horizon 2020 Programme (H2020/2014–2020) under grant agreement no. 767533. This publication reflects only the author's view, exempting the Community from any liability. Project web site: https://www.ensureal.com/ (accessed on 1 October 2017).

Institutional Review Board Statement: Not applicable.

Informed Consent Statement: Not applicable.

Data Availability Statement: The data presented in this study are available within the article and in supplementary materials.

Conflicts of Interest: The authors declare no conflict of interest and the funders had no role in the design of the study; in the collection, analyses, or interpretation of data; in the writing of the manuscript, or in the decision to publish the results.

References

1. Balomenos, E.; Davris, P.; Pontikes, Y.P.D.; Delipaltas, A. Bauxite Residue Handling Practice and Valorisation Research in Aluminium of Greece. In Proceedings of the 2nd International Bauxite Residue Valorisation and Best Practices Conference, Athens, Greece, 7–10 May 2018; pp. 29–38.
2. Miller, J.; Irgens, A. Alumina Production by the Pedersen Process—History and Future. In *Essential Readings in Light Metals*; Donaldson, D., Raahauge, B.E., Eds.; Springer International Publishing: Cham, Switzerland, 2016; pp. 977–982.
3. Hosteman, J.W.; Patterson, S.H.; Good, E.E. *World Nonbauxite Aluminum Resources Excluding Alunite*; 1076C; United States Department of Energy: Washington, DC, USA, 1990.
4. Vafeias, M.; Marinos, D.; Panias, D.; Safarian, J.; Van Der Eijk, C.; Solhem, I.; Davris, P. From red to grey: Revisiting the Pedersen process to achieve holistic bauxite ore utilisation. In Proceedings of the 2nd International Bauxite Residue Valorisation and Best Practices Conference, Athens, Greece, 7–10 May 2018; pp. 111–117.
5. Nielsen, K. The Pedersen Process—An old process in a new light. *Erzmetall* **1978**, *31*, 523–525.
6. Barr, L.F.K. Alumina production from andalusite by the Pedersen process. *Trans. Inst. Min. Metall. Sect. C Miner. Process. Extr. Metall.* **1977**, *86*, C64–C70.
7. Lazou, A.; Van Der Eijk, C.; Tang, K.; Balomenos, E.; Kolbeinsen, L.; Safarian, J. The Utilization of Bauxite Residue with a Calcite-Rich Bauxite Ore in the Pedersen Process for Iron and Alumina Extraction. *Metall. Mater. Trans. B* **2021**, *52*, 1255–1266. [CrossRef]

8. Hignett, T. PILOT PLANTS: Production of Alumina from Clay by a Modified Pedersen Process. *Ind. Eng. Chem.* **1947**, *39*, 1052–1060. [CrossRef]
9. Pedersen, H. Process of Manufacturing Aluminum Hydroxide. U.S. Patent 1,618,105, 15 February 1927.
10. Aktieselskapet Norsk Aluminium. Process for the Manufacture of Aluminium Oxide. U.S. Patent 252,399, 9 June 1927.
11. Peter William Reynolds Laurence Roy Pittwell Ici Ltd. Improvements in and Relating to the Production of Alumina. U.S. Patent GB-667145-A, 26 October 1949.
12. Thomson, M.R.; McLeod, H.M.J.; Skow, M.L. *Recovery of Alumina from Submarginal Bauxites—Part. 2.—Extraction of Alumina from Electric-Furnace Slags of Calcium Aluminate*; United States Department of the Interior-Bureau of Mines: Washington, DC, USA, 1949.
13. Copson, R.L.; Walthall, J.H.; Hignett, T.P. *Aluminum-Extraction of Alumina from Clays by the Lime-Sinter Modification of the Pedersen Process*; The American Institute of Mining, Metallurgical, and Petroleum Engineers: New York, NY, USA, 1944.
14. Shayanfar, S.; Aghazadeh, V.; Saravari, A.; Hasanpour, P. Aluminum hydroxide crystallization from aluminate solution using carbon dioxide gas: Effect of temperature and time. *J. Cryst. Growth* **2018**, *496*, 1–9. [CrossRef]
15. Aghazadeh, V.; Shayanfar, S.; Samiee Beyragh, A. Thermodynamic Modeling and Experimental Studies of Bayerite Precipitation from Aluminate Solution: Temperature and pH Effect. *Iran. J. Chem. Chem. Eng.* **2019**, *38*, 229–238. [CrossRef]
16. Aghazadeh, V.; Shayanfar, S.; Hassanpour, P. Aluminum hydroxide crystallization from aluminate solution using carbon dioxide gas: Effect of pH and seeding. *Miner. Process. Extr. Metall.* **2019**. [CrossRef]
17. Blake, H.E. *Adaptation of the Pedersen Process to the Ferruginous Bauxites of the Pacific Northwest*; Department of the Interior, Bureau of Mines: Washington, DC, USA, 1967.
18. Wang, Z.; Yang, L.; Zhang, J.; Guo, Z.-C.; Zhang, Y. Adjustment on gibbsite and boehmite co-precipitation from supersaturated sodium aluminate solutions. *Trans. Nonferrous Met. Soc.* **2010**, *20*, 521–527. [CrossRef]
19. Li, Y.; Zhang, Y.; Yang, C.; Zhang, Y. Precipitating sandy aluminium hydroxide from sodium aluminate solution by the neutralization of sodium bicarbonate. *Hydrometallurgy* **2009**, *98*, 52–57. [CrossRef]
20. Panov, A.; Senyuta, A.; Smirnov, A.; Pechenkin, M. Revisiting alternative smelter grade alumina production processes. In Proceedings of the TMS 2021, Virtual, Pittsburgh, PA, USA, 15–18 March 2021.
21. Safarian, J.; Kolbeinsen, L. Sustainability in alumina production from bauxite. In Proceedings of the 2016 Sustainable Industrial Processing Summit and Exhibition, Flogen, Hainan-Island, China, 6–10 November 2016.
22. Padilla, R.; Sohn, H.Y. Sodium aluminate leaching and desilication in lime-soda sinter process for alumina from coal wastes. *Metall. Trans. B* **1985**, *16*, 707–713. [CrossRef]
23. Li, Y.; Lei, T.; Yang, D.J. Radionuclide of Process of Carbon Decomposition and Anneal of Liquor after Desilication from Nepheline. *Appl. Mech. Mater.* **2013**, *330*, 22–26. [CrossRef]
24. Wojcik, M.; Pyzalski, M. Factors effecting on the properties of bayerite obtained in the carbonization process of alkaline aluminate solutions. In Proceedings of the Light Metals 1990 AIME Annual Meeting, Anaheim, CA, USA, 18–22 February 1990; pp. 161–165.
25. Zhou, Q.; Peng, D.; Peng, Z.; Liu, G.; Li, X. Agglomeration of gibbsite particles from carbonation process of sodium aluminate solution. *Hydrometallurgy* **2009**, *99*, 163–169. [CrossRef]
26. Lee, M.-Y.; Parkinson, G.M.; Smith, P.G.; Lincoln, F.J.; Reyhani, M.M. Characterization of Aluminum Trihydroxide Crystals Precipitated from Caustic Solutions. In *Separation and Purification by Crystallization*; ACS Symposium Series; American Chemical Society: Washington, DC, USA, 1997; Volume 667, pp. 123–133.
27. Stewart, J.J. Comparison of the accuracy of semiempirical and some DFT methods for predicting heats of formation. *J. Mol. Model.* **2004**, *10*, 6–12. [CrossRef] [PubMed]
28. Tettenhorst, R. Crystal Chemistry of Boehmite. *Clays Clay Miner.* **1980**, *28*, 373–380. [CrossRef]
29. Sato, T.; Sato, K. Preparation of Gelatinous Aluminium Hydroxide from Aqueous Solutions of Aluminium Salts Containing Sulphate Group with Alkali. *J. Ceram. Soc. Jpn.* **1996**, *104*, 377–382. [CrossRef]
30. Nail, S.L.; White, J.L.; Hem, S.L. Comparison of IR spectroscopic analysis and X-ray diffraction of aluminum hydroxide gel. *J. Pharm. Sci* **1975**, *64*, 1166–1169. [CrossRef]
31. Bardossy, G.; White, J.L. Carbonate inhibits the crystallization of aluminum hydroxide in bauxite. *Science* **1979**, *203*, 355–356. [CrossRef]
32. Serna, C.J.; Lyons, J.C.; White, J.L.; Hem, S.L. Stabilization of aluminum hydroxide gel by specifically adsorbed carbonate. *J. Pharm. Sci* **1983**, *72*, 769–771. [CrossRef]
33. Koga, N.; Fukagawa, T.; Tanaka, H. Preparation and Thermal Decomposition of Synthetic Bayerite. *J. Therm. Anal. Calorim.* **2001**, *64*, 965–972. [CrossRef]
34. Balan, E.; Blanchard, M.; Hochepied, J.-F.; Lazzeri, M. Surface modes in the infrared spectrum of hydrous minerals: The OH stretching modes of bayerite. *Phys. Chem. Miner.* **2008**, *35*, 279–285. [CrossRef]
35. Wolska, E.; Szajda, W. Use of infrared spectroscopy to identify crystalline aluminum hydroxides of the $Al(OH)_3$-$Fe(OH)_3$ system. *J. Appl. Spectrosc.* **1983**, *38*, 137–140. [CrossRef]
36. Sato, T.; Yamashita, T.; Ozawa, F. The Preparation of Bayerite from sodium aluminate solutions with carbon dioxide. *Z. Für Anorg. Allg. Chem.* **1969**, *370*, 202–208. [CrossRef]
37. Jraba, N.; Tounsi, H.; Makhlouf, T. Valorization of Aluminum Chips into γ-Al_2O_3 and η-Al_2O_3 with High Surface Areas via the Precipitation Route. *Waste Biomass Valorization* **2016**, *9*, 1003–1014. [CrossRef]

38. Zolfaghari, R.; Rezai, B.; Bahri, Z.; Mahmoudian, M. Influences of New Synthesized Active Seeds and Industrial Seed on the Aluminum Hydroxide Precipitation from Sodium Aluminate Solution. *J. Sustain. Metall.* **2020**, *6*, 643–658. [CrossRef]
39. Jodin-Caumon, M.C.; Humbert, B.; Phambu, N.; Gaboriaud, F. A vibrational study of the nature of hydroxyl groups chemical bonding in two aluminium hydroxides. *Spectrochim Acta A Mol. Biomol. Spectrosc.* **2009**, *72*, 959–964. [CrossRef] [PubMed]
40. White, J.L.; Hem, S.L. Role of carbonate in aluminum hydroxide gel established by Raman and IR analyses. *J. Pharm. Sci.* **1975**, *64*, 468–469. [CrossRef] [PubMed]
41. Le Bozec, N.; Persson, D.; Nazarov, A.; Thierry, D. Investigation of Filiform Corrosion on Coated Aluminum Alloys by FTIR Microspectroscopy and Scanning Kelvin Probe. *J. Electrochem. Soc.* **2002**, *149*, B403–B408. [CrossRef]
42. Kiss, A.B.; Keresztury, G.; Farkas, L. Raman and i.r. spectra and structure of boehmite (γ-AlOOH). Evidence for the recently discarded D172h space group. *Spectrochim. Acta Part A Mol. Spectrosc.* **1980**, *36*, 653–658. [CrossRef]
43. Russell, J.D.; Farmer, V.C.; Lewis, D.G. Lattice vibrations of boehmite (γ-AlOOH): Evidence for a C122v rather than a D172h space group. *Spectrochim. Acta Part A Mol. Spectrosc.* **1978**, *34*, 1151–1153. [CrossRef]
44. Alex, T.C.; Kailath, A.J.; Kumar, R. Al-Monohydrate (Boehmite) to Al-Trihydrate (Bayerite/Gibbsite) Transformation during High-Energy Milling. *Metall. Mater. Trans. B* **2020**, *51*, 443–451. [CrossRef]
45. Sato, T. Preparation of aluminium hydroxide by reacting sodium aluminate solutions with mineral acid. *J. Chem. Technol. Biotechnol.* **2007**, *31*, 670–675. [CrossRef]
46. Panias, D.; Krestou, A. Effect of synthesis parameters on precipitation of nanocrystalline boehmite from aluminate solutions. *Powder Technol.* **2007**, *175*, 163–173. [CrossRef]
47. Panias, D.; Paspaliaris, I. *Precipitation of Boehmite—An Innovative Route in the Alumina Production*; National Technical University of Athens: Athens, Greece, 1998.
48. Czajkowski, A.; Noworyta, A.; Krótki, M. Studies and modelling of the process of decomposition of aluminate solutions by carbonation. *Hydrometallurgy* **1981**, *7*, 253–261. [CrossRef]
49. Krestou, A.; Panias, D. *Alumina Hydrate Precipitates in the System $NaAl(OH)_4$ (Supersaturated)/HNO_3*; National Technical University of Athens: Athens, Greece, 2005; Volume 4.
50. Bradley, S.M.; Kydd, R.A.; Howe, R.F. The Structure of Al Gels Formed through the Base Hydrolysis of Al^{3+} Aqueous Solutions. *J. Colloid Interface Sci.* **1993**, *159*, 405–412. [CrossRef]
51. Li, H.; Addai-Mensah, J.; Thomas, J.C.; Gerson, A.R. The crystallization mechanism of $Al(OH)_3$ from sodium aluminate solutions. *J. Cryst. Growth* **2005**, *279*, 508–520. [CrossRef]
52. Gates-Rector, S.; Blanton, T. The Powder Diffraction File: A quality materials characterization database. *Powder Diffr.* **2019**, *34*, 352–360. [CrossRef]